Resonant impurity scattering and electron-phonon scattering in the electrical resistivity of Cr thin films

Z. Boekelheide,* David W. Cooke, E. Helgren, and F. Hellman
Department of Physics, University of California, Berkeley, California 94720, USA
(Received 22 May 2009; published 29 October 2009)

The resistivity as a function of temperature from 0.6 to 300 K for epitaxial and polycrystalline Cr thin films is presented and fit to a model which includes electron-phonon scattering and resonant impurity scattering. Resonant impurity scattering from localized defect states in the spin-density wave gap leads to very high residual resistivity (up to 400 $\mu\Omega$ cm) and a minimum at low temperatures (below 100 K). This is strong experimental evidence for resonant impurity scattering due to defects in pure Cr rather than dopant atoms. The magnitude of the resistivity minimum scales linearly with the residual resistivity over 2 orders of magnitude. At moderate temperatures (100–300 K) the resistivity shows a positive, linear temperature dependence due to electron-phonon scattering. Defects affect the electron-phonon scattering as well leading to a variation in the effective Debye temperature and resistivity slope between samples, a significant deviation from Matthiessen's rule.

DOI: 10.1103/PhysRevB.80.134426 PACS number(s): 75.30.Fv, 72.10.Di, 73.61.−r, 72.10.Fk

I. INTRODUCTION

Bulk chromium is an itinerant antiferromagnet with an incommensurate spin-density wave (ISDW) and has been widely studied as an archetypal band antiferromagnet.[1] The SDW in bulk Cr is very sensitive to perturbation by dopant atoms, pressure, etc. In particular, the ISDW switches to a commensurate SDW with the addition of a few percent Mn and disappears altogether with the addition of V. A large body of research exists on the effects of various dopants in Cr.[2–13]

In addition to changing the SDW state, dopant atoms lead to interesting features in the resistivity. These features are described by the theory of resonant impurity scattering, which results from itinerant antiferromagnetism. The theory predicts localized impurity states within the "forbidden" SDW gap. When those states exist near the Fermi energy, resonant scattering occurs. In the prototypical system, $Cr_{1-y-x}Fe_y(Mn,V)_x$, resistivity minima and residual resistivities up to 25 $\mu\Omega$ cm have been observed; the effect is attributed to resonant impurity scattering off of the Fe impurities, with Mn and V (+1 and −1 valencies compared to Cr) used to tune the Fermi level through the impurity energy levels.[3–7] Resistivity minima due to resonant scattering have also been seen in many binary Cr alloys, including Cr-V, Cr-Mo, Cr-Al, Cr-Ge, and Cr-Si.[2] Recently, more detailed resistivity analyses including the effect of resonant impurity scattering have been performed on Cr-Si, Cr-Fe, Cr-Ga-(Mn,V), and Cr-Ru-V.[8–11]

Theoretically, the type of impurity atom is not very important to formation of a localized state, and even defects in pure Cr should lead to resonant impurity scattering.[3] This has never been observed in bulk samples, presumably because the density of defects is very small. However, polycrystalline Cr films provide many defects in the form of grain boundaries, point defects, and dislocations. Defects and strain found in polycrystalline Cr films have already been shown to cause changes in the SDW state: an infrared reflectivity study of the SDW gaps in Cr films showed that Cr films have incommensurate, commensurate, or mixed SDW states depending on film-deposition conditions.[14]

In the literature, Cr thin films have been shown to have very high resistivities,[14–17] but with little to no explanation of the reason. Thornton and Hoffman[15] showed that the room-temperature resistivity of sputtered Cr films increases strongly with increased sputtering gas pressure, up to an extremely high value of 2000 $\mu\Omega$ cm; they attributed the high resistivity to a structure of columnar grains with low-density grain boundaries, a structure that is often observed when low-Z materials are sputtered at high sputtering gas pressure. However, such high resistivities are not observed for similar materials such as Fe under the same deposition conditions.[18]

In addition to defect and impurity scattering, electron-phonon scattering is a significant contribution to the resistivity. According to Matthiessen's rule, the addition of defects and impurities should add a temperature-independent term to the resistivity without affecting the temperature-dependent electron-phonon resistivity.[19] We suggest this is an overly simplistic assumption in the case of Cr. Not only do defects and impurities add a temperature-dependent term to the resistivity due to resonant impurity scattering, but electron-phonon scattering, which contributes the linear term to the resistivity, can also be affected by defects. A recent specific-heat study of polycrystalline sputtered Cr films found a decrease in the Debye temperature from the bulk value due to a softening of the lattice. There was also an increase in the electronic specific-heat coefficient γ for samples grown at high sputtering pressure which is explained by a disorder broadening induced increase in the electron density of states $N(E_F)$ and a resultant increase in the electron-phonon coupling constant λ.[20] Both of these effects would be expected to impact Matthiessen's rule.

In this paper, we present the temperature-dependent resistivities of epitaxial and polycrystalline Cr thin films. We fit the resistivity curves to a model which includes electron-phonon scattering and resonant impurity scattering in the temperature range below 150 K where the contribution to the resistivity from magnetic fluctuation scattering around the

 ©2009 The American Physical Society

Neel temperature is negligible. The films are presented in three series. First, we present a series of three films grown by electron beam (e-beam) evaporation on different substrates with varying degrees of epitaxy to test the effect of epitaxy and grain boundaries on the resistivity. Next, we present a series of polycrystalline sputtered films grown at different sputtering pressures which varies the columnar morphology as described above.[15] Finally, we present a series of annealed films, taking the highest resistivity film and annealing it at a series of temperatures in order to better understand the nature of the defects in these films.

II. EXPERIMENT

The first series of films was grown by e-beam evaporation at a rate of 0.3 Å/s and a base pressure below 5×10^{-8} Torr. The films in this series were grown at the same time onto three different substrates: MgO (001), Al_2O_3 (0001) (c-plane sapphire), and amorphous SiO_2-coated Si, held at 300 °C during growth. Cr is well known to grow epitaxially, in the (001) orientation, on MgO (001).[21] The Cr lattice constant is approximately $\sqrt{2}$ smaller than the MgO lattice constant, causing the film to grow 45° rotated from the MgO. Cr exhibits (011) textured growth on Al_2O_3 (0001) induced by epitaxy. The epitaxy occurs in nine distinct orientation relationships, leading to a polycrystalline film with grains of the different orientations.[22,23] Finally, Cr grows polycrystalline, without a specific orientation, on the a-SiO_2/Si.

Reflection high-energy electron diffraction (RHEED) of Cr on MgO during growth shows a streaky pattern, consistent with two-dimensional epitaxial growth. X-ray diffraction (XRD) shows a strong Cr (001) peak, with no other orientations, in a θ-2θ scan. In a ϕ scan (azimuthal scan) of the 45° off-axis Cr (011) peak, fourfold symmetry is observed, confirming epitaxy. For Cr growth on Al_2O_3 (0001), RHEED shows a spotty pattern, which suggests three-dimensional (3D) epitaxial growth, and only the Cr (011) peak is seen in an XRD θ-2θ scan. A ϕ scan of the 45° off-axis Cr (002) peak showed six broad peaks, consistent with the nine orientation relations described in the literature.[24] The Cr/a-SiO_2/Si sample was grown on an amorphous substrate and therefore has no epitaxy. A θ-2θ scan of the Cr/a-SiO_2/Si sample showed all three allowed bcc diffraction peaks, (002), (011), and (112), suggesting a polycrystalline film with no preferred orientation. The width of the peaks suggests an out-of-plane correlation length of 30 nm.

Top-down scanning electron microscopy (SEM), in Figs. 1(a) and 1(b), shows that both the Cr/Al_2O_3 and the Cr/a-SiO_2/Si samples consist of elongated grains about 17 nm × 50 nm in size. The epitaxial Cr/MgO sample had no surface structure visible by SEM.

The sputtered series of samples was grown in an AJA magnetron sputtering system with a base pressure below 5×10^{-8} Torr. The gun was powered with 150 W dc, and the films were deposited at rates of 0.5–1.0 Å/s onto substrates of amorphous SiN_x/Si held at room temperature. The Ar sputtering gas pressure was varied between 0.75 and 8 mTorr. In addition to this series, one sample was sputtered at

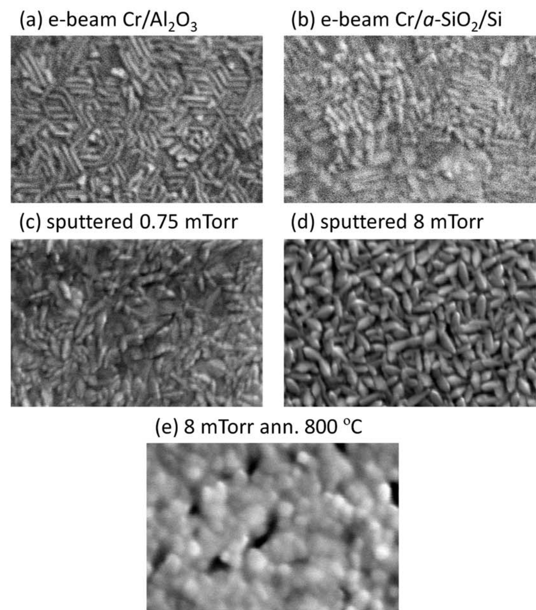

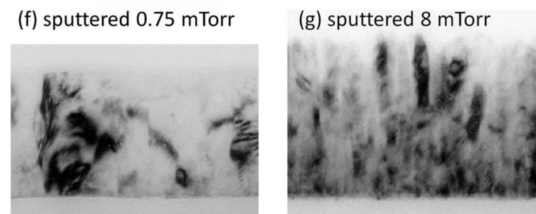

FIG. 1. [(a)–(e)] SEM top-down images of samples: (a) e-beam deposited Cr/Al_2O_3, (b) e-beam deposited Cr/a-SiO_2/Si, (c) sputtered 0.75 mTorr, (d) sputtered 8 mTorr, and (e) sputtered 8 mTorr annealed at 800 °C. [(f) and (g)] Cross-sectional TEM images: (f) sputtered 0.75 mTorr (100 nm film) and (g) sputtered 8 mTorr (130 nm film).

0.75 mTorr with the substrate held at 350 °C; this sample had larger grains and exhibited bulklike behavior, including a clear ISDW,[14] and this will be referred to as the "bulklike" sample for the rest of the paper.

The sputtering gas pressure plays an important role in the growth kinetics of sputtered films—low Ar pressure leads to high-energy incident atoms, while high pressure leads to thermalization and lower incident energy. This results in high- and low-pressure sputtered films having drastically different morphologies. Cross-sectional transmission electron microscopy (TEM), in Figs. 1(f) and 1(g), shows that both high- and low-pressure films have columnar structure. The low-pressure films are flat and exhibit high tensile stress, while the high-pressure films are very rough, have low tensile stress, and have wide grain boundaries which include some amorphous material. SEM, in Figs. 1(c) and 1(d), shows that the grains are oblong and about 25 nm × 35 nm for the 0.75 mTorr film and 25 nm × 50 nm for the 8 mTorr film. The correlation length from x-ray diffraction for the room-temperature sputtered samples ranged from 18 to 28 nm and was 35 nm for the bulklike sample. More

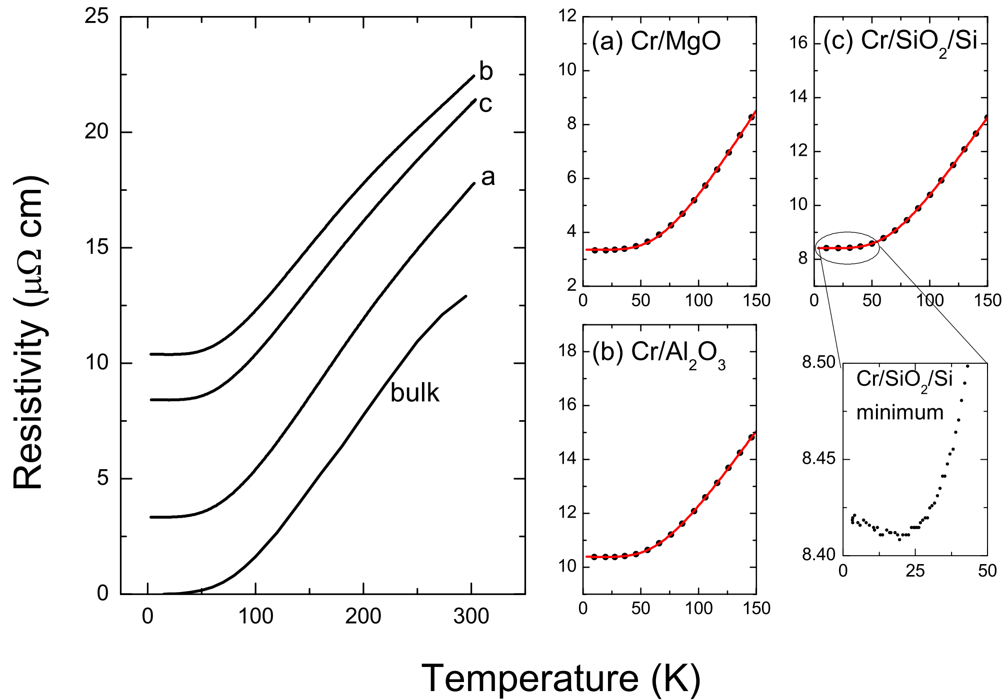

FIG. 2. (Color online) Resistivity as a function of temperature for e-beam deposited Cr films grown on three substrates with varying degrees of epitaxy: MgO (epitaxial single crystal), Al_2O_3 (textured polycrystalline), and SiO_2/Si (untextured polycrystalline). Bulk data is from White and Woods (Ref. 26). In the closeup panels, selected data points are shown with the least-squares fits to Eq. (6).

details of the growth and characterization of these sputtered samples are given elsewhere.[14]

The very high resistivity seen in some of these films is unusual and naturally raises the question of impurities in the film. To study this, we chose the most resistive sample, the 8 mTorr sputtered sample (392 $\mu\Omega$ at 5 K), and annealed it at a series of temperatures. A rapid thermal annealer was used, with an Ar atmosphere, to anneal the sample at 400, 600, and 800 °C for 2 minutes each. A factor of 10 decrease in the resistivity with annealing at 800 °C suggests that the reason for the high resistivity is, in fact, crystal defects which can be removed by annealing rather than impurity atoms. SEM done on the annealed samples showed little change in grain structure with annealing to 400 and 600 °C but a significant change after annealing at 800 °C. The grains of the annealed sample are round as opposed to oblong and there are some large voids which may have been formed when smaller voids between grains coalesced during the annealing process [Fig. 1(e)].

Energy dispersive x-ray spectroscopy (EDS) found no Ar, N, or C contamination in the films, within the margin of error of 0.25 at. % for Ar and N and 1.0 at. % for C.[25] Total oxygen percentage was 2 at. % in the sputtered films grown at low pressure and 4 at. % in the films grown at high pressure. Chromium is known to form a self-limiting oxide and these results are consistent with a surface oxide layer given that the films grown at high pressure were rough and had about twice the surface area to oxidize.

All films described here are approximately 200 nm, so that differences between films can be attributed to deposition conditions rather than thickness differences. Actual thickness, used to calculate resistivity, was measured with a KLA-Tencor Alpha-Step IQ profilometer or a KLA-Tencor Nanopics AFM with an uncertainty in thickness of approximately 2%.

The films were patterned so the geometry was well defined. Resistivity was measured using a dc four-point probe method to avoid contact resistance effects.

III. RESULTS

Resistivity as a function of temperature for the three series of samples is presented in Figs. 2–4. Each figure shows the resistivity of all samples in the series on one plot. Individual plots of the low-temperature resistivity for each sample are also shown with a least-squares fit to the data described in Sec. IV.

The three main features to note in the resistivity are the residual resistivity (ρ_0), the minimum in the resistivity at low temperatures due to resonant impurity scattering, and the linear slope of the resistivity at moderate temperatures due to electron-phonon scattering. The most commonly studied feature in the resistivity of Cr is the Neel transition which occurs at T_N=310 K in bulk Cr and ranges from 220 to >400 K in our films.[14] We will not discuss the Neel transition here, and instead focus on the resonant impurity scattering and electron-phonon scattering features at low and moderate temperatures.

The resistivity vs temperature curves for the films in the e-beam deposited series are shown in Fig. 2. In these films, all three resistivity features vary between samples. The residual resistivity is very low (3.4 $\mu\Omega$ cm) for the epitaxial film on MgO and increases for the polycrystalline samples, both the textured Cr/Al_2O_3 (10.4 $\mu\Omega$ cm) and untextured

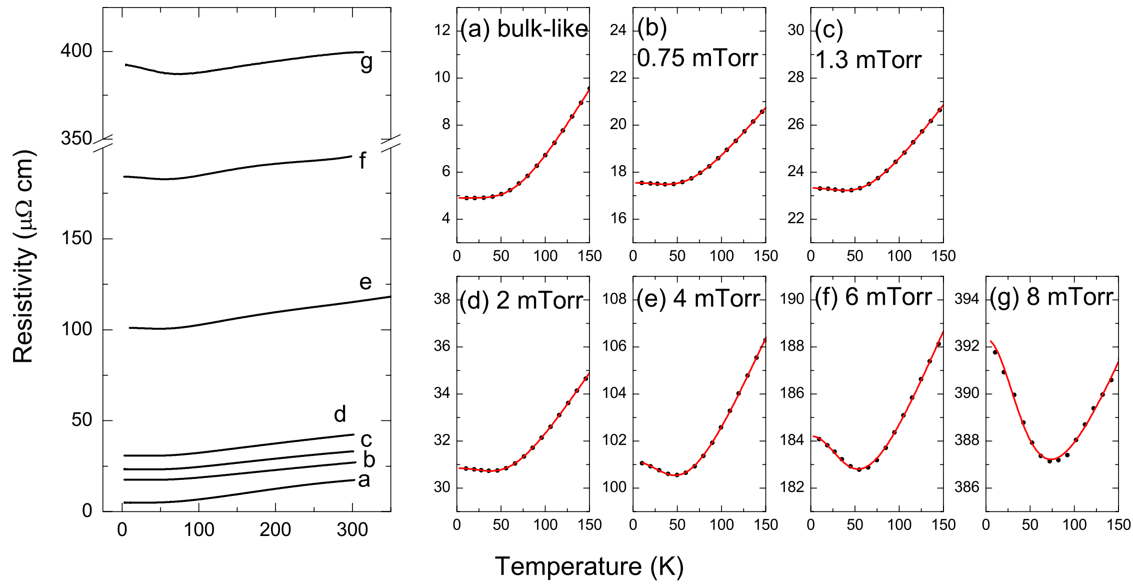

FIG. 3. (Color online) Resistivity as a function of temperature for unannealed sputtered films grown at different sputtering pressures. In the closeup panels, selected data points are shown with the least-squares fits to Eq. (6).

Cr/a-SiO$_2$/Si (8.4 $\mu\Omega$ cm). This is expected, as grain boundaries cause scattering. At low temperatures, a minimum in the resistivity is observed for all three samples; it is shown in a closeup of the low-temperature data for the Cr/a-SiO$_2$/Si film in Fig. 2. This minimum is due to resonant scattering from defects in the film. Finally, the slope of the resistivity at moderate temperatures also varies between samples; it is very close to bulk for the Cr/MgO sample and lower for the Cr/Al$_2$O$_3$ and Cr/a-SiO$_2$/Si samples. Both the resistivity minima and the difference in resistivity slope between samples are deviations from Matthiessen's rule which states that resistivity vs temperature curves should be parallel for samples of the same material with different amounts of defects.[19]

The resistivity vs temperature curves are shown in Fig. 3 for the series of sputtered samples. The range of low-temperature resistivities observed in these samples is significantly larger than in the previous series of samples, increasing from 4.9 to 392 $\mu\Omega$ cm with increasing sputtering pressure. The resonant scattering minimum increases drasti-

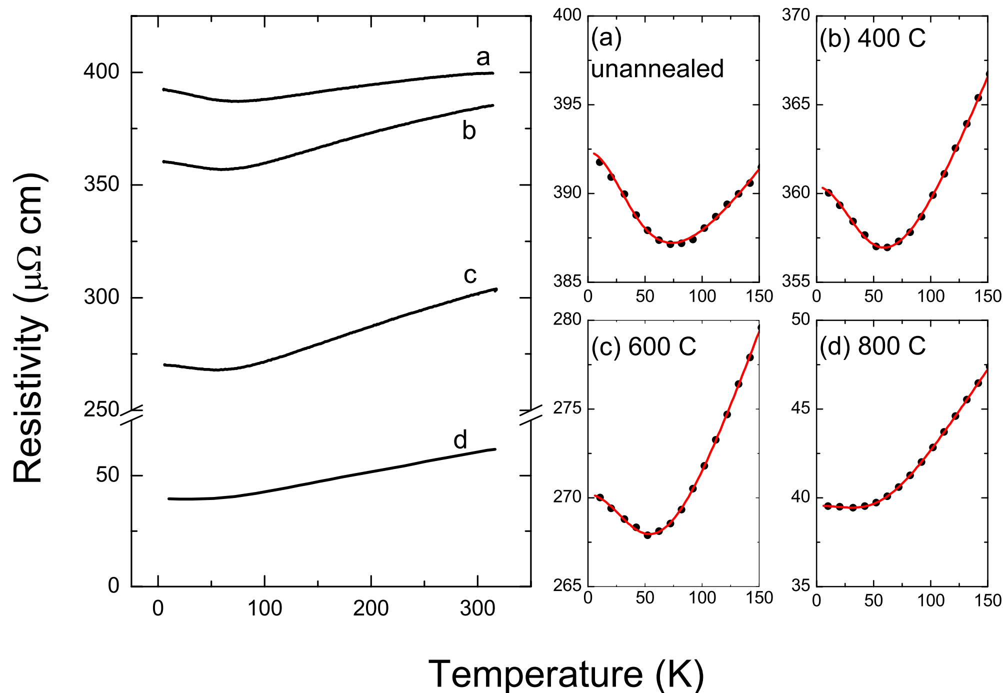

FIG. 4. (Color online) Resistivity as a function of temperature for a film sputtered at 8 mTorr and then annealed at a series of temperatures. In the closeup panels, selected data points are shown with the least-squares fits to Eq. (6).

cally with sputtering pressure as well, with the depth of the minimum as large as 5 $\mu\Omega$ cm for the highest resistivity (8 mTorr) sample. One film, the 1.3 mTorr sample, was measured to as low as 0.6 K in order to investigate the low-temperature limit of the resistivity minimum. It was found that the increase in resistivity at low-temperatures levels off as $T\to 0$. This excludes the possibility of insulating behavior being responsible for the minimum as that would cause the resistivity to increase infinitely upon approaching 0 K. The slope of the resistivity in these films varies as well, although the variation in slope is much smaller than the variation in the residual resistivity.

The film with resistivity of 392 $\mu\Omega$ cm at 5 K, the 8 mTorr sputtered film, was annealed at a series of temperatures. The resistivity vs temperature profiles are shown in Fig. 4. Both the residual resistivity and the magnitude of the resistivity minimum are decreased by annealing. The most dramatic effect is seen for the 800 °C annealed film, in which the low-temperature resistivity decreases by a factor of 10, from 392 to 39 $\mu\Omega$ cm. This is a clear indication that both the high residual resistivity and the observed resistivity minima are primarily due to defects in the crystal which are eliminated by annealing. In this series, the slope of the resistivity also varies significantly, increasing in the 400 and 600 °C samples and then decreasing again in the 800 °C sample. The reasons for the nonmonotonic behavior of the slope are not obvious, and are left for the discussion in Sec. V.

IV. MODEL FOR THE RESISTIVITY

The resistivity of Cr can be written as a sum of multiple terms. Following the work of Chiu *et al.*,[12] we write:

$$\rho(T) = \rho^{res}(T) + \frac{\rho_0 + \rho_{e-p}(T) + \rho_m(T)}{1 - \alpha\Delta(T)/\Delta(0)}. \quad (1)$$

Here, $\rho^{res}(T)$ is the resistivity due to resonant impurity scattering, ρ_0 is the residual resistivity due to normal potential scattering, $\rho_{e-p}(T)$ is the resistivity due to electron-phonon scattering, and $\rho_m(T)$ is the resistivity due to magnetic fluctuations. The term $1-\alpha\Delta(T)/\Delta(0)$ accounts for the decrease in the number of carriers at the Fermi surface below T_N due to the SDW gap. $\Delta(T)$ is the SDW gap and α is the fraction of carriers at the Fermi surface that is destroyed by the SDW gap.

The films in this paper are sufficiently thick (200 nm) that they are considered 3D systems. In addition, the thickness is significantly larger than the mean free path, so we do not take surface scattering into account. Electron-electron scattering is also not significant for our model.[27,28]

This equation can be simplified considerably by considering only temperatures well below T_N. The function $\Delta(T)$ has the form of a BCS gap; well below T_N, $1-\alpha\Delta(T)/\Delta(0) \to 1-\alpha$. The resistivity due to fluctuation scattering, ρ_m, contributes a maximum of 1.5 $\mu\Omega$ cm to the resistivity at T_N, and becomes negligible below about $0.5T_N$. For temperatures below $0.75T_N$, ρ_m is less then 5% of the phonon resistivity.[12] We will apply the fit from 2–150 K, which is less than $0.5T_N$ for most samples and less than $0.75T_N$ for all samples, so that $\rho_m \to 0$.

Making these simplifications with the assumption that T is well below T_N, we are left with a resistivity that takes the following form:

$$\rho(T) = \rho^{res}(T) + \frac{\rho_0}{1-\alpha} + \frac{\rho_{e-p}(T)}{1-\alpha}. \quad (2)$$

α for bulk Cr is 0.3 and varies from 0.3–0.55 in Cr alloys.[12,13] Because the SDW is known to vary between thin-film samples grown under different deposition conditions, it is possible that α varies as well. Rather than assuming a numerical value for $1-\alpha$, we redefine ρ_0 and $\rho_{e-p}(T)$ to include the $1-\alpha$ term

$$\rho(T) = \rho_0 + \rho^{res}(T) + \rho_{e-p}(T). \quad (3)$$

The temperature-dependent resonant term, $\rho^{res}(T)$, takes the following form:[3]

$$\rho^{res}(T) = \frac{\rho_0^{res}}{1 + (T/\Theta_{res})^2}, \quad (4)$$

where ρ_0^{res} is the magnitude of the resonant scattering minimum and Θ_{res} is a parameter related to the energy width of the localized states leading to resonant scattering and the energy difference between these states and the Fermi energy. The shape of this function is such that the resistivity varies as $-T^2$ at low temperatures, increasing as the temperature is decreased but leveling off as $T\to 0$.

The term $\rho_{e-p}(T)$ can be written as a Bloch-Gruneisen function, which is derived from the Debye model for phonons. This term goes as T^n at low temperatures and as T at moderate to high temperatures; the crossover between the two is related to the Debye temperature of the material.

$$\rho_{e-p}(T) = C_G \frac{T^n}{\Theta_G^{n+1}} \int_0^{\Theta_G/T} \frac{x^n}{(e^x - 1)(1 - e^{-x})} dx. \quad (5)$$

Here, C_G is a constant and Θ_G is an effective Debye temperature.

For simple metals $n=5$ due to phonon-mediated *s*-*s* intraband transitions. However, in the transition metals it is often seen that $n=3$ because *s*-*d* interband transitions dominate. Generally, the $n=5$ form of Eq. (5) is known as the Bloch Gruneisen function, while the lesser known $n=3$ form is attributed to Wilson.[29] In Cr, both *s*-*s* and *s*-*d* scattering occur.

Least-squares fits applied to our data for the epitaxial Cr/MgO film, which has low residual resistivity of 3 $\mu\Omega$ cm and a negligible resistivity minimum (0.003 $\mu\Omega$ cm deep), show that the $n=5$ form fits significantly better than $n=3$ based on χ^2. A plot of the ideal resistivity of the epitaxial Cr/MgO sample (with ρ_0 subtracted) is given in Fig. 5 with both the $n=5$ and 3 forms of Eq. (5). The residuals of both fits are shown as well. Although the fits of Eq. (5) with $n=5$ are very good, there is some noticeable systematic deviation at low temperatures. The actual resistivity of Cr/MgO at low temperatures increases more quickly than the fit with $n=5$, but more slowly than $n=3$. The residuals of the two fits oppose each other, which implies that a fit of a linear combination of the two terms would be optimal. To avoid over-

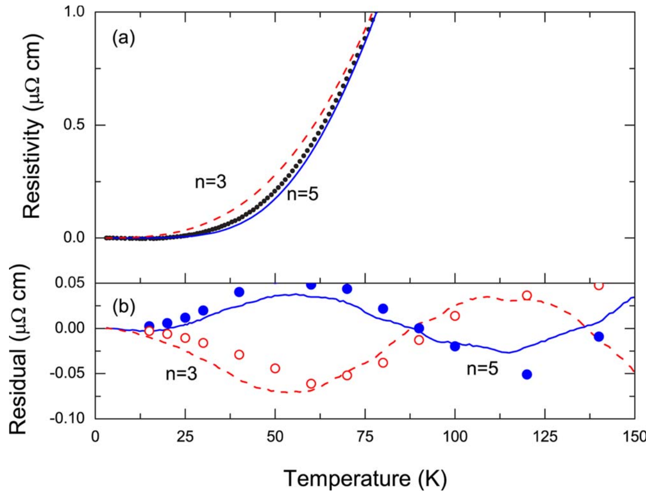

FIG. 5. (Color online) (a) The ideal resistivity of the epitaxial Cr/MgO sample (points), fit to the $n=5$ and 3 forms Eq. (5) (solid and dashed lines). The residual resistivity has been subtracted from the data so that only the electron-phonon term in the resistivity is fit resulting in two parameters, C_G and Θ_G. (b) Lines: the residuals of the $n=5$ (solid) and 3 (dashed) fit for the Cr/MgO samples. Points: the residuals of the $n=5$ (solid) and 3 (empty) fit for ideal bulk Cr resistivity from White and Woods (Ref. 26).

parameterization, we chose to use only the dominant $n=5$ (s-s scattering) to fit the remaining data sets. The maximum residual of the $n=5$ fit is 0.04 $\mu\Omega$ cm, which we take as the minimum error in our fit parameters. The residuals of $n=5$ and 3 fits to the bulk data from White and Woods[26] were very similar, suggesting that the epitaxial Cr/MgO sample is a good comparison to bulk.

Aside from the choice of n, there is another assumption made in using the Bloch-Gruneisen function: the Debye model. The Debye model assumes that the phonon dispersion relation $\omega(k)$ is linear, and the maximum phonon energy gives the Debye temperature Θ_D. In reality, $\omega(k)$ is not linear and has structure. This is often described within the Debye model by stating $\Theta_D(T)$ as a variable which depends on temperature.[30,31] In Cr, the value for $\Theta_D(0)$ is quoted as 585 K,[20,32] while $\Theta_D(\infty)$ is quoted as 478 K.[30] The Bloch-Gruneisen function uses an average value for the Debye temperature; to avoid confusion we call this Θ_G. The effect of using an average value rather than a temperature-dependent $\Theta_D(T)$ should cause the fit resistivity to increase more quickly at low temperature. However, in Fig. 5 it is clear that the fit increases more slowly than the data. Thus, the effect of using a temperature average of $\Theta_D(T)$ on the electron-phonon resistivity is smaller than the effect of s-d scattering.

With the assumption of dominant s-s scattering, Eq. (2) can be written

$$\rho(T) = \rho_0 + \frac{\rho_0^{res}}{1+(T/\Theta_{res})^2} + C_G \frac{T^5}{\Theta_G^6}\int_0^{\Theta_G/T} \frac{x^5}{(e^x-1)(1-e^{-x})}dx. \tag{6}$$

We applied a least-squares fit of Eq. (6) to the resistivity data from 2 to 150 K. For the error bars on the fit parameters we used the error in the fit given by origin 8 added in quadrature to the error in the fit to the Bloch-Gruneisen function due to s-d scattering (0.04 $\mu\Omega$ cm, the maximum residual to the fit shown in Fig. 5). There is also a 2% overall uncertainty in $\rho(T)$ due to the thickness measurement which is not included in the error in the fit parameters. As might be expected for a five-parameter fit, the error bars are large in some cases. In particular, for the samples with very slight minima, the parameters describing the minimum, ρ_0^{res} and Θ_{res}, have large error bars. Likewise, the samples with very pronounced minima have large errors in the parameter Θ_G because the Bloch-Gruneisen behavior is obscured by the large minimum. However, the resulting fit closely matches the data for every sample, including bulk data.

V. DISCUSSION

The fit parameters for all three series of samples are tabulated in Table I. The five fit parameters are: ρ_0, the residual resistivity; ρ_0^{res}, the magnitude of the resonant scattering minimum; Θ_{res}, the resonant scattering energy parameter; Θ_G, the Debye temperature; and $C_G/4\Theta_G^2$, the slope of the linear term in the electron-phonon resistivity. Also shown are the values of Θ_G and $C_G/4\Theta_G^2$ for bulk ideal ($\rho_0=0$) resistivity from White and Woods,[26] obtained from a fit to only the electron-phonon term in the model.

We have chosen to present the Bloch-Gruneisen prefactor as $C_G/4\Theta_G^2$ because as $T\rightarrow\infty$,

$$\rho_{e-p}(T) \rightarrow \frac{C_G}{4\Theta_G^2}T. \tag{7}$$

Thus, $C_G/4\Theta_G^2 = d\rho/dT$ in the high-temperature limit of the Bloch-Gruneisen function. This is a very good approximation for high temperatures ($T \gtrsim 1.5\Theta_G$). For moderate temperatures ($0.2\Theta_G \lesssim T \gtrsim 1.5\Theta_G$), where the resistivity appears linear in temperature, the slope of the Bloch-Gruneisen function actually deviates from $C_G/4\Theta_G^2$ by as much as 20%. Thus, the parameter $C_G/4\Theta_G^2$ obtained from a fit of the Bloch-Gruneisen function at low and moderate temperatures is the best way to compare high-temperature resistivity slopes between samples with different Θ_G without necessitating measurement of the resistivity above $1.5\Theta_G$ (about 700 K) which would anneal the samples and alter their properties.

A. Residual resistivity ρ_0

The behavior of ρ_0 in these samples is qualitatively logical, increasing with the presence of defects and grain boundaries. ρ_0 increases substantially with sputtering pressure, as seen in Fig. 6, due to the morphology of wide grain boundaries with many defects observed in films grown at high pressure. There is a significant decrease in ρ_0 for films that are either annealed or grown epitaxially, which decreases the number of defects.

Quantitatively, the magnitude over which ρ_0 varies is anomalously large. Fe films grown under the same sputtering conditions, which have similar microstructure to Cr films due to the similar atomic masses and look similar in SEM im-

TABLE I. Table of parameters derived from a least-squares fit of each sample's resistivity to Eq. (6), for the three sample series. ρ_0—residual resistivity, ρ_0^{res}—magnitude of resonant resistivity minimum, Θ_{res}—resonant scattering energy parameter, Θ_G—Debye temperature, $C_G/4\Theta_G^2$—linear resistivity slope (high temperature). There is an overall 2% uncertainty in $\rho(T)$ which is not shown in the table due to uncertainty in the thickness measurement.

	Sample	ρ_0 ($\mu\Omega$ cm)	ρ_0^{res} ($\mu\Omega$ cm)	Θ_{res} (K)	Θ_{B-G} (K)	$C_{B-G}/4\Theta_{B-G}^2$ ($\mu\Omega$ cm/K)
	Bulk ideal ρ (White and Woods[b])				519 ± 17	0.054 ± 0.004
E-beam series: vary substrate						
E-beam deposited onto 300 °C substrates	epitaxial Cr/MgO	3.4 ± 0.04			464 ± 11	0.055 ± 0.002
	highly textured Cr/Al_2O_3	10.4 ± 0.05			450 ± 5	0.0488 ± 0.0003
	untextured $Cr/a\text{-}SiO_2/Si$	8.4 ± 0.04			450 ± 3	0.0505 ± 0.0004
Sputtered series: vary pressure						
Polycrystalline sputtered onto room temp a-SiN_x substrates	bulklike[a]	4.9 ± 0.04			468 ± 8	0.050 ± 0.001
	0.75 mTorr	16.9 ± 0.2	0.6 ± 0.2	86 ± 18	432 ± 7	0.037 ± 0.002
	1.3 mTorr	22.6 ± 0.2	0.7 ± 0.2	75 ± 12	429 ± 8	0.041 ± 0.002
	2 mTorr	30.0 ± 0.2	0.8 ± 0.2	73 ± 12	420 ± 8	0.046 ± 0.003
	4 mTorr	98.6 ± 0.6	2.5 ± 0.6	65 ± 11	407 ± 18	0.071 ± 0.010
	6 mTorr	179.7 ± 1.4	4.5 ± 1.3	60 ± 11	384 ± 37	0.077 ± 0.026
	8 mTorr	381.6 ± 1.3	10.7 ± 1.3	57 ± 5	400 ± 44	0.080 ± 0.031
Annealed series: vary anneal temp						
8 mTorr sputtered sample annealed	unannealed	381.6 ± 1.3	10.7 ± 1.3	57 ± 5	400 ± 44	0.080 ± 0.031
	400 °C	350.9 ± 1.4	9.5 ± 1.4	60 ± 6	408 ± 27	0.139 ± 0.029
	600 °C	262.6 ± 1.7	7.6 ± 1.7	64 ± 9	417 ± 25	0.153 ± 0.031
	800 °C	39.2 ± 0.1	0.4 ± 0.1	40 ± 6	419 ± 5	0.079 ± 0.001

[a]Sputtered at 0.75 mTorr onto a 350 °C substrate.
[b]Reference 26.

ages, have also been shown to have increasing ρ_0 with pressure, but the effect is significantly smaller. An 8 mTorr sputtered Fe film has ρ_0 of 42 $\mu\Omega$ cm, almost ten times smaller than ρ_0 for the 8 mTorr Cr film.[18] The primary cause of the high resistivity in Cr films is resonant scattering from localized states within the SDW gap, a unique result of the itinerant antiferromagnetism.

Typical amorphous transition-metal alloys have ρ_0 around 150 $\mu\Omega$ cm because they generally have about one carrier electron per atom and the mean free path is on the order of

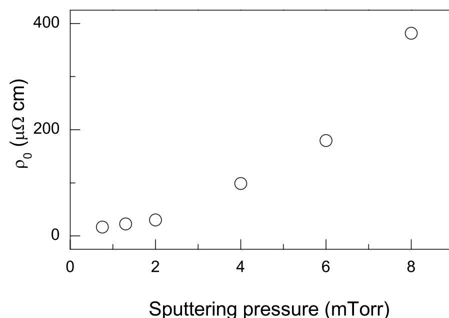

FIG. 6. ρ_0 as a function of sputtering pressure, for the sputtered samples. Error bars are smaller than the symbol size.

the interatomic spacing. Generally, the resistivity of alloys with ρ_0 lower than this increases with temperature (positive $d\rho/dT$). As ρ_0 approaches 150 $\mu\Omega$ cm, $d\rho/dT$ decreases, this behavior is called saturation and is thought to be due to the failure of the Boltzmann transport model when the mean free path is on the order of the interatomic spacing. Alloys with ρ_0 higher than this threshold tend to have a negative $d\rho/dT$, due to quantum backscattering.[33] This is not a steadfast rule, but a correlation (often called the Mooij correlation) which is observed in a wide range of alloys.

Exceptions to this are "bad metals" which exhibit positive $d\rho/dT$ up to resistivities well beyond 150 $\mu\Omega$ cm, corresponding to mean free paths decreasing continuously through one interatomic spacing and lower, a nonphysical result. Examples are the high T_c superconductors, and the colossal magnetoresistance manganates. Although the materials exhibiting bad-metal behavior are often exotic, the same transport behavior can be produced in good metals if their geometry is constricted. This effect has been reported in thin silver films in the regime where silver islands begin to coalesce.[34] If only a few of the silver islands in a film are touching, the electrons must take a longer, tortuous path through the film, changing the effective length of the sample. When converting the measured resistance to resistivity, this results in a

multiplicative factor (l_{eff}/l) in the resistivity. The signature of such a geometry effect is that $d\rho/dT$ increases proportionally with ρ_0.

The Cr 8 mTorr sample has $\rho_0=381.6$ $\mu\Omega$ cm, which assuming 0.25 holes per electron,[35,36] corresponds to a mean free path of about 4.3 Å. This is a very small mean free path for a film with a grain size of 280 Å, but is slightly larger than the lattice constant, so it is not truly a bad metal. Still, this high resistivity could be partially explained by a geometry effect such as the one observed in the silver films. If some regions of the high-pressure samples are not conducting (for example, the "valleys" between columnar grains, some of the grain boundaries, or voids within the sample), this would constrict the path of the conduction electrons, introducing a multiplicative factor l_{eff}/l into the resistivity.

For our Cr films, the slope $C_G/4\Theta_G^2$ varies considerably between samples for reasons other than geometry (see Sec. V C) and therefore cannot be used as a test for the geometry factor l_{eff}/l in the same way. An Fe film sputtered at 8 mTorr, under the same conditions showed a geometric factor l_{eff}/l of about 3 in the resistivity based on a 3× increased resistivity slope, while a 2 mTorr film showed no geometry enhancement. The factor l_{eff}/l should be similar for these films due to the similar microstructure; therefore we attribute to the Cr 8 mTorr film a factor l_{eff}/l of 3, and an unknown geometry factor between 1 and 3 for the 4 and 6 mTorr samples. This leaves an intrinsic resistivity of 130 $\mu\Omega$ cm and a slope ($C_G/4\Theta_G^2$) of 0.27 $\mu\Omega$ cm for our 8 mTorr Cr film. These are plausible values for ρ_0 within the Mooij correlation and for $C_G/4\Theta_G^2$ within the range of our data on other polycrystalline films, however, a ρ_0 of 130 $\mu\Omega$ cm, which corresponds to a 12.9 Å mean free path, is still unusually high.

Resonant scattering, which causes the resistivity minimum, also causes very high residual resistivity. Theoretically, the resistivity due to resonant scattering is entirely accounted for by the expression for $\rho^{res}(T)$ shown in Eq. (4), while ρ_0 represents nonresonant scattering. Based on our fit for the 8 mTorr sample, for example, the resonant scattering term accounts for about 10 $\mu\Omega$ cm of the total resistivity at 2 K, while the nonresonant part ρ_0 accounts for the other 382 $\mu\Omega$ cm. In practice, the residual resistivity in resonant scattering systems is generally much higher than would be expected based on the form of $\rho^{res}(T)$. For the prototypical incommensurate resonant scattering system, $Cr_{0.985-x}Fe_{0.015}V_x$, ρ_0 is about 12 $\mu\Omega$ cm. The magnitude of the resistivity minima due to resonant scattering varies between samples, but a typical value is about 0.3 $\mu\Omega$ cm. Assuming that ρ_0 and the depth of the resonant scattering minimum scale linearly with the number of resonant scatterers, an approximately 10 $\mu\Omega$ cm resistivity minimum such as is seen in the 8 mTorr sample would correspond to a residual resistivity of about 400 $\mu\Omega$ cm, approximately what we observe. Thus, the very high residual resistivity seen in our samples is consistent with resonant scattering.

A linear correlation between the magnitude of the resonant scattering minimum ρ_0^{res} and ρ_0 in our samples is shown in Fig. 7. Such a correlation is not surprising but the range over which it persists is. In the literature resonant scattering is typically studied by keeping the number of scatterers constant (e.g., Fe 1.5 at. % for incommensurate or 2.7 at. % for commensurate) while varying the Fermi level (x at. % Mn or V). As such, little data exist on the concentration dependence of the resonant scattering minimum. Our results show a linear correlation between ρ_0^{res} and ρ_0 which is maintained over 2 orders of magnitude.

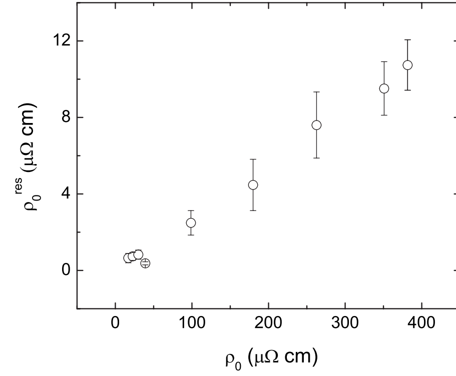

FIG. 7. Linear correlation between the magnitude of the resonant scattering resistivity minimum ρ_0^{res} and the residual resistivity ρ_0.

B. Resonant impurity scattering minimum (ρ_0^{res} and Θ_{res})

Two samples, the e-beam deposited epitaxial Cr/MgO and sputtered bulklike Cr, had negligible low-temperature minima (less than 0.005 $\mu\Omega$ cm) and the resonant scattering term in the five-parameter fit did not converge, so the parameters listed in Table I are those for a three-parameter fit of ρ_0 plus electron-phonon scattering. Two samples, the e-beam deposited textured polycrystalline Cr/Al_2O_3 sample and untextured polycrystalline $Cr/a\text{-}SiO_2/Si$, have minima which were fit to the five-parameter model but the size of the minima given by the parameter ρ_0^{res} is within the error of the fit. Therefore, for these two samples both fit parameters of the resonant term must be considered statistically insignificant within this model.

In the theory of resonant impurity scattering, the energies of the localized states within the gap depend on the type of impurity as well as the type of SDW in the Cr matrix. In the case of a commensurate SDW, a small concentration of an impurity ion is expected to lead to two localized states within the SDW, symmetric about the middle of the gap. In the case of an incommensurate SDW there is expected to be a continuum of localized energy levels within the gap with some structure to it which causes the resonance.[7] In samples known to be commensurate, tuning the Fermi energy (through Mn or V doping) leads to a peak in the residual resistivity when the Fermi energy falls at the energy of one of the localized states. In addition, commensurate samples not only show the expected resistivity minimum at low temperatures, but sometimes also exhibit a resistivity maximum at even lower temperatures. This maximum is due to the fact that the energies of the localized states within the gap also have a temperature dependence.[6] Incommensurate samples do not show such a maximum; because the energy levels are spread out within the gap, a small temperature dependence of

the energy levels does not have a significant effect.

The resistivity behavior in our Cr thin films suggests localized states that are spread out within the gap. Although our samples are known to have varied SDW states (commensurate, incommensurate, and mixed),[14] no maxima are observed in the low-temperature resistivity. In addition, the variation in both ρ_0^{res} and ρ_0 within each series of films is monotonic. If the states occurred at only two energies within the gap, varying a parameter such as sputtering pressure (which varies the strain within the sample, which in turn varies the Fermi energy) should lead to a peak in ρ_0^{res} and ρ_0 when the Fermi energy is tuned to the localized state. However, it is possible that such a peak would not be observable amidst the very strong dependence of ρ_0^{res} and ρ_0 on the number of defects in the films. One way to explain the states being spread out inside the gap is that the defects leading to localized states can take many forms. For example, single vacancies, interstitials, vacancy clusters, dislocations, and multiple types of grain boundaries. Along a single grain boundary, even, each atom experiences a different potential due to its position. This distribution of defects and potentials would lead to multiple different sets of energy levels, resulting in a distribution of localized states within the SDW gap even for samples with a commensurate SDW.

Resonant scattering states should be observable in the specific heat as an increase in the density of states at the Fermi energy $N(E_F)$. Specific-heat measurements of sputtered Cr films showed that $N(E_F)$ increases for the high sputtering pressure samples.[20,37] This can be explained by disorder broadening, because the Fermi energy of Cr lies at a minimum in the density of states. If the broadened states fall inside the SDW gap, they will become localized, according to theory.[3] The observed $N(E_F)$ for high sputtering pressure samples is higher than not only bulk antiferromagnetic Cr but also paramagnetic Cr, which has about 50% higher $N(E_F)$ than antiferromagnetic Cr due to the disappearance of the SDW gap. If the increase in $N(E_F)$ for the sputtered samples were due to simple band broadening due to disorder, this would obliterate the SDW gap and cause the films to be paramagnetic. However, infrared reflectivity measurements have shown that the SDW still exists in these films. This suggests that rather than simple band broadening which would completely erase the SDW gap, the band broadening is more complicated: states are shifted to the SDW gap from above and below and are localized, while the SDW is maintained.

Besides resonant scattering, other possible explanations for a minimum in the resistivity are insulating grain boundaries or the Kondo effect. Insulating grain boundaries would lead to an exponential temperature dependence of the resistivity at low temperatures, which we do not observe. The Kondo effect, however, leads to a $-T^2$ temperature dependence of the resistivity at low temperatures, the same as for resonant scattering. In antiferromagnetic Cr with impurities, low-temperature minima have been explained by resonant impurity scattering, and are not believed to be due to the Kondo effect for multiple reasons. First, resistivity minima have been seen in systems for which the impurity atom is known to be nonmagnetic in Cr, and second, the SDW should suppress the spin-flip scattering of conduction electrons which is responsible for the Kondo effect. In paramagnetic Cr samples (>3 at. % V) with magnetic impurities, resistivity minima have been observed and are thought to be due to the Kondo effect.[6] Our resistivity analysis cannot distinguish between resonant scattering and the Kondo effect, however, based on the known antiferromagnetism in our films[14] and the large density of states at the Fermi energy observed in the specific-heat study,[20] resonant impurity scattering is the most likely explanation.

The parameter Θ_{res} is related to both the energy width of the localized state within the SDW gap which causes resonant scattering and the difference in energy between these states and the Fermi level. We find Θ_{res} to be similar for all films with a slight decreasing trend with ρ_0. The similar values for all films implies similar scattering centers in these films. The differences between films are primarily due to the *number* of scatterers rather than the type. Furthermore, the linear relation between ρ_0^{res} and ρ_0, discussed in Sec. V A and shown in Fig. 7, also supports the idea that the observed differences in resonant scattering between films are primarily due to the number of scatterers and not the type.

The 8 mTorr, 800 °C annealed sample has a significantly lower value for Θ_{res} than the others. This signifies a difference in the type of defects contributing to scattering in the 800 °C sample. The residual resistivity of this film is still somewhat high and must be due to defects which are not removed by annealing at 800 °C or, possibly, impurities incorporated during the annealing process. Thus, the localized scattering state within the SDW gap should be different as well, leading to a different Θ_{res}.

C. Electron-phonon scattering (Θ_G and $C_G/4\Theta_G^2$)

The fit parameters of the Bloch-Gruneisen function can elucidate the nature of electron-phonon interaction in the Cr films. The effective Debye temperature, Θ_G, for bulk Cr, obtained from the Bloch-Gruneisen model, is 519 K, while the values observed in the films vary between 384 and 468 K. This is a significant decrease from bulk, which can be explained by "phonon softening"—a change in the phonon density of states which effectively decreases the average phonon energy at each temperature. Phonon softening in sputtered Cr thin films has also been observed in specific-heat measurements.[20,37] The value of Θ_G in these Cr films correlates well to ρ_0, suggesting that the phonon softening can be attributed to disorder. In Fig. 8, we present a plot of Θ_G vs ρ_0. Θ_G rapidly decreases upon initially adding defects. As more defects are added to the system, the effect of each defect on Θ_G declines, suggesting that the majority of phonon softening occurs at a relatively low threshold for disorder.

$C_G/4\Theta_G^2$ is equivalent to the high-temperature slope $d\rho/dT$ of the Bloch-Gruneisen function, which by Matthiessen's rule is expected to remain constant between different samples of the same material with different concentrations of impurities and defects. In reality, many factors contribute to $d\rho/dT$ and can vary between samples. Table I shows $C_G/4\Theta_G^2$ for all samples varying between 0.037 and 0.153 $\mu\Omega$ cm/K, with no clear correlation to ρ_0 or any other variable.

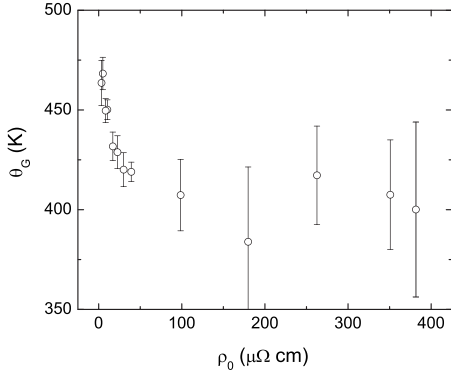

FIG. 8. Correlation between the effective Debye temperature Θ_G and the residual resistivity ρ_0.

The slope $d\rho/dT$ can be directly related to the transport electron-phonon coupling constant λ_{tr}

$$d\rho/dT = \frac{2\pi m k_B}{ne^2\hbar}\lambda_{tr}. \qquad (8)$$

The transport electron-phonon coupling constant differs from the specific-heat electron-phonon coupling constant λ by an angular factor (the integral of $1-\cos\theta$) which is close to 1. Thus, $d\rho/dT$ is often used as a measure of the electron-phonon coupling constant.[38]

Specific-heat studies of the sputtered Cr films showed an increase in both $N(E_F)$ and λ for high-pressure sputtered samples (4 and 8 mTorr). An increase in λ should show up in the resistivity as an increase in $d\rho/dT$. However, an increase in $N(E_F)$ could compensate for an increase in λ if the additional states are charge carriers contributing to n. As discussed previously, additional states that occur at k values inside the SDW gap become localized and cause resonant scattering. Additional states outside the SDW gap are not localized, and therefore can contribute to conduction. Assuming that all the additional states outside the SDW gap contribute to conduction, and assuming α, the fraction of the Fermi surface destroyed by the SDW, is 0.3, then using the values for λ calculated from the specific-heat experiments[20] for the 8 mTorr sample $d\rho/dT$ would increase by a factor of 1.25 and for the 4 mTorr sample $d\rho/dT$ would increase by a factor of 1.10.

These values for the increase in $d\rho/dT$ due to the increased λ are lower limits. First, α may vary from the bulk value of 0.3; for Cr alloys it ranges from about 0.3–0.55. A larger α would increase the number of additional states in $N(E_F)$ which are localized and therefore do not contribute to conduction, decreasing the amount by which $N(E_F)$ contributes to an increase to n, compensating for the increase in λ. Or, if some of the additional states outside the SDW gap do not contribute very much to conduction, for example, if they are more d-like than s-like, this would also decrease the amount by which $N(E_F)$ contributes to an increase in n. In either case, the increase in $d\rho/dT$ would be larger than the estimates above.

Besides λ and $N(E_F)$, we will show that there are other factors which affect the resistivity slope, and therefore $d\rho/dT$ cannot be used as an independent measure of λ_{tr} for these samples.

First, Eq. (8) for $d\rho/dT$ refers to the intrinsic resistivity. For the high-pressure sputtered films, the geometry effect discussed in Sec. V A increases the measured (extrinsic) resistivity by a factor of l_{eff}/l from the intrinsic resistivity. For the 8 mTorr sample, l_{eff}/l is taken to be three based on results for Fe films. For the 4 and 6 mTorr films, l_{eff}/l is expected to be somewhere between 1 and 3.

Secondly, we experimentally observe an effect which decreases $d\rho/dT$ for samples containing grain boundaries. The e-beam deposited series of samples can elucidate the role of grain boundaries in $C_G/4\Theta_G^2$. The epitaxial Cr/MgO sample has very good single-crystal epitaxy by RHEED and XRD, and this is the sample which has $C_G/4\Theta_G^2$ closest to that of bulk Cr. As grain boundaries are introduced, in the Cr/Al_2O_3 and $Cr/a\text{-}SiO_2/Si$ films, the slope is decreased somewhat, suggesting that grain boundaries cause a decrease in $C_G/4\Theta_G^2$ from the bulk value.

In the sputtered series of samples, $C_G/4\Theta_G^2$ for the low-pressure films is also below the bulk value. The bulklike sample, which has larger grains due to the elevated growth temperature, has the value closest to bulk. $C_G/4\Theta_G^2$ is only higher than bulk for the high-pressure 4, 6, and 8 mTorr films which are known or suspected to have a geometry factor l_{eff}/l enhancing the measured $d\rho/dT$ above its intrinsic value. For the 8 mTorr film, taking l_{eff}/l into account, the intrinsic $d\rho/dT$ is 0.028 $\mu\Omega$ cm/K, even lower than that of the low-pressure films. The physical mechanism for this decrease in slope with grain boundaries is not understood at this time.

For the annealed films, $C_G/4\Theta_G^2$ behaves nonmonotonically with annealing temperature. In the as-grown state, this sample, prepared at high pressure (8 mTorr) has a slope above bulk. Annealing to 400 and 600 °C increases the slope significantly, by about a factor of 2. Upon annealing to 800 °C, however, the residual resistivity is significantly decreased, and the slope is reduced. This nonmonotonic behavior is likely due to competition between various effects on the slope. As the film is annealed, the geometry factor l_{eff}/l likely decreases due to grain growth and healing of defects, effectively reducing the measured $d\rho/dT$. At the same time, grain growth should reduce the effect of the grain boundary effect discussed above, which should increase $d\rho/dT$.

The magnitudes of the various effects on $d\rho/dT$ can only be estimated after making serious assumptions about the nature of the additional states in $N(E_F)$, the fraction of the Fermi surface destroyed by the spin-density wave (α), and the geometry factor l_{eff}/l. Because the physical mechanism behind the decrease in $d\rho/dT$ due to grain boundaries is not understood, its magnitude cannot be accounted for. The multiple competing effects make it impossible to extract the individual components of $d\rho/dT$ and calculate λ_{tr}.

VI. CONCLUSION

We have shown the temperature-dependent resistivities of epitaxial and polycrystalline Cr thin films and fit the data to a model which includes electron-phonon scattering and reso-

nant impurity scattering. The resistivity of Cr thin films is decidedly more complex than the parallel curves expected from Matthiessen's rule, which assumes that defects simply add a temperature-independent term to the resistivity. We observe multiple temperature-dependent effects due to defects in our films.

Localized defect states within the SDW gap lead to resonant scattering in Cr films, causing a very large residual resistivity in some samples and a resistivity minimum at low temperatures. The magnitude of the minimum, ρ_0^{res}, is proportional to ρ_0 over 2 orders of magnitude, suggesting that most of the contribution to ρ_0 is due to resonant scattering. In addition, the resonant scattering energy parameter Θ_{res} is similar for films grown under varying conditions, suggesting that the type of localized state formed by defects is similar for all films. The resonant scattering in these films is due to defects in pure Cr rather than dopant atoms.

Defects also lead to changes in the electron-phonon resistivity, causing the effective Debye temperature Θ_G to decrease due to phonon softening. The slope of the resistivity in the linear regime varies between samples due a combination of extrinsic geometry, grain boundaries, and changes in the electron-phonon coupling and number of electrons at the Fermi energy.

ACKNOWLEDGMENTS

The authors thank Aidin Fathalizadeh and Ivan Borzenets for assistance and David J. Smith from Arizona State University for the TEM. This work was supported by the U.S. Department of Energy under Contract No. DE-AC02-05CH11231.

---

*zboekelheide@berkeley.edu

[1] E. Fawcett, Rev. Mod. Phys. **60**, 209 (1988).

[2] E. Fawcett, H. L. Alberts, V. Yu. Galkin, D. R. Noakes, J. V. Yakhmi, Rev. Mod. Phys. **66**, 25 (1994).

[3] B. A. Volkov and V. V. Tugushev, Sov. Phys. Solid State **26**, 1471 (1984).

[4] V. Yu Galkin, V. V. Tugushev, and T. E. Tugusheva, Sov. Phys. Solid State **28**, 1282 (1986).

[5] V. Yu Galkin, Fiz. Met. Metalloved. **64**, 1199 (1987).

[6] V. Yu Galkin and T. E. Tugusheva, Sov. Phys. Solid State **30**, 487 (1988).

[7] V. Yu Galkin and T. E. Tugusheva, Sov. Phys. Solid State **31**, 1626 (1989).

[8] A. R. E. Prinsloo, H. L. Alberts, and P. Smit, J. Phys.: Condens. Matter **10**, 2715 (1998).

[9] K. T. Roro, A. R. E. Prinsloo, and H. L. Alberts, J. Alloys Compd. **393**, 16 (2005).

[10] A. R. E. Prinsloo, H. A. Derrett, H. L. Alberts, and A. M. Venter, J. Appl. Phys. **99**, 08F706 (2006).

[11] L. Reddy, H. L. Alberts, A. M. Strydom, A. R. E. Prinsloo, and A. M. Venter, J. Appl. Phys. **103**, 07C903 (2008).

[12] C. H. Chiu, M. H. Jericho, and R. H. March, Can. J. Phys. **49**, 3010 (1971).

[13] J. O. Strom-Olsen, D. F. Wilford, and A. P. Morris, J. Phys. F: Met. Phys. **12**, 1247 (1982).

[14] Z. Boekelheide, E. Helgren, and F. Hellman, Phys. Rev. B **76**, 224429 (2007).

[15] J. A. Thornton and D. W. Hoffman, J. Vac. Sci. Technol. **14**, 164 (1977).

[16] A. K. Kulkarni and L. C. Chang, Thin Solid Films **301**, 17 (1997).

[17] M. A. Angadi and L. A. Udachan, J. Mater. Sci. **16**, 1412 (1981).

[18] A. Fathalizadeh and Z. Boekelheide, Berkeley Scientific **11**, 29 (2007).

[19] J. Bass, Adv. Phys. **21**, 431 (1972).

[20] D. W. Cooke, Z. Boekelheide, D. R. Queen, and F. Hellman, J. Appl. Phys. **105**, 07C314 (2009).

[21] E. E. Fullerton, S. D. Bader, and J. L. Robertson, Phys. Rev. Lett. **77**, 1382 (1996).

[22] T. Wagner, Q. Fu, C. Winde, S. Tsukimoto, and F. Phillipp, Interface Sci. **12**, 117 (2004).

[23] S. Tsukimoto, F. Phillipp, and T. Wagner, J. Eur. Ceram. Soc. **23**, 2947 (2003).

[24] A ϕ scan of the 45° off-axis (001) peak in a single crystal (011) oriented film should yield two peaks. In the literature it is suggested that two types of orientation relationships occur in Cr growth on Al_2O_3 (0001): ORI with three orientations in plane (yielding six peaks) and ORII with six orientations in plane (yielding twelve peaks), 5.26° offset from ORI in either direction, for a total of nine orientation relationships and eighteen peaks in the azimuthal scan. However, the broad peaks observed in our diffraction pattern as well as in the literature cannot distinguish between ORI and ORII 5.26° apart so only six peaks are observed.

[25] An additional film was grown on a Si thermal oxide substrate so at. % N could be measured without observing a signal from the SiN_x substrate. For at. % C, the EDS chamber had a background 5 at. % C signal which obscured the measurement; the margin of error for the at. % C measurement is therefore 1%.

[26] G. K. White and S. B. Woods, Philos. Trans. R. Soc. London, Ser. A **251**, 273 (1959).

[27] A T^2 term in the resistivity due to electron-electron scattering has never been quantified for Cr, however an estimate based on the isoelectronic element W finds the magnitude of the electron-electron scattering resistivity significantly less than the residual in the Bloch-Gruneisen fit at low temperatures (0.0006 $\mu\Omega$ cm at 15 K) and dwarfed by the electron-phonon scattering term at moderate to high temperatures (1% of the electron-phonon resistivity at 150 K).

[28] J. S. Dugdale, *The Electrical Properties of Metals and Alloys* (Edward Arnold, London, 1977).

[29] G. T. Meaden, *Electrical Resistance of Metals* (Plenum, New York, 1965), p. 89.

[30] J. L. Feldman, Phys. Rev. B **1**, 448 (1970).

[31] J. A. Rayne and W. R. G. Kemp, Philos. Mag. **1**, 918 (1956).

[32] F. Heiniger, E. Bucher, and J. Muller, Phys. Kondens. Mater. **5**, 243 (1966).
[33] J. H. Mooij, Phys. Status Solidi A **17**, 521 (1973).
[34] S. B. Arnason, S. P. Herschfield, and A. F. Hebard, Phys. Rev. Lett. **81**, 3936 (1998).
[35] Y. Furuya, J. Phys. Soc. Jpn. **40**, 490 (1976).
[36] S. Foner, Phys. Rev. **107**, 1513 (1957).
[37] B. Revaz, M.-C. Cyrille, B. L. Zink, I. K. Schuller, and F. Hellman, Phys. Rev. B **65**, 094417 (2002).
[38] G. Grimvall, Phys. Scr. **14**, 63 (1976).